Eur Biophys J (1996) 24: 348–353

BIOPHYSICS LETTER

Frank G. Schmidt · Florian Ziemann · Erich Sackmann

Shear field mapping in actin networks by using magnetic tweezers

Received: 8 February 1996 / Accepted in revised form: 29 March 1996

Abstract An improved magnetic bead microrheometer based on phase contrast microscopy allowing high resolution measurements of local deformations within macromolecular networks is applied to study local viscoelastic properties of cross-linked actin networks. By embedding non-magnetic colloidal beads as probes into the networks, the spatial variation of the strain field within cross-linked actin networks can be mapped. Moreover, the Poisson ratio and shear modulus can be measured locally.

Key words Biogels · actin networks · magnetic tweezers · microrheology of polymer networks · cytoskeleton viscoelasticity

Introduction

Macromolecular networks of biological materials such as the actin-based cell cytoskeleton and the extracellular matrix are often heterogeneous on a micrometer scale which is essential for their biological function (Darnell et al. 1990). Depending on the spatial variation of (1) the length distribution of the actin filaments, (2) the F-actin polymer volume fraction and (3) the degree of cross-linking, the cytoskeleton elasticity may vary by orders of magnitude within a cell (Wachsstock et al. 1993) and this heterogeneity is essential for the local force generation during cell locomotion (cf. Stossel 1994) or the local stabilisation of cell adhesion (cf. Schindl et al. 1995). The development of micromechanical techniques for local measurements of viscoelastic properties or forces generated by molecular motors is an important and challenging task of cell biophysics. Recent progress in the development of micromechanical techniques for local force measurements within soft materials such as optical tweezers (Kuo and Sheetz 1992; Svoboda et al. 1993), magnetic bead microrheometers (Zaner and Valberg 1989; Wang et al. 1993; Ziemann et al. 1994), micropipette techniques (Evans et al. 1995) or glass fiber force measuring devices (Ishijima et al. 1991) open new possibilities for local quantitative measurements of elastic and rheological properties of cell membranes or of the cytoskeleton and allow direct measurements of molecular force generation in molecular motors (Finer et al. 1994).

In the present work we report a new method allowing the direct visualisation and evaluation of shear fields in macromolecular networks. The method is based on the local application of a point force generated by magnetic tweezers and the analysis of the deformation in the neighbourhood of a magnetic bead by tracking the local motions of non-magnetic colloidal probes embedded in the network. The time dependent viscoelastic response of the probes in the direction parallel and perpendicular to the force can be recorded and the Poisson ratio and shear modulus of the gels can be directly measured locally.

Experimental setup and deformation analysis

The magnetic bead rheometer ("magnetic tweezers") described previously (Ziemann et al. 1994) has been improved in several ways. Figure 1 shows a schematic view of the experimental setup which is mounted on a Zeiss Axiovert microscope. Larger magnetic coils (diameter: 2 cm; length: 4 cm; 1600 turns of 0.35 mm copper wire) with soft iron cores have been built to increase the magnetic field and to allow the additional use of oil immersion microscopy. The maximum force which can be generated by these coils on a 4.5 μm Dynabead in the middle of the sample cell (that is, at a distance of 4 mm from the tips of the iron cores) is about 20 pN. The sample cells consist of cylindrical plexiglass tubes (outer diameter: 8 mm). The actual compartment containing the actin network (see magnifica-

F. G. Schmidt · F. Ziemann · E. Sackmann[1] (✉)
Physics Department E22 (Biophysics Group),
Technische Universität München, James-Franck-Strasse,
D-85747 Garching, Germany

On leave:
[1] Institute for Theoretical Physics,
University of California, Santa Barbara, California, USA

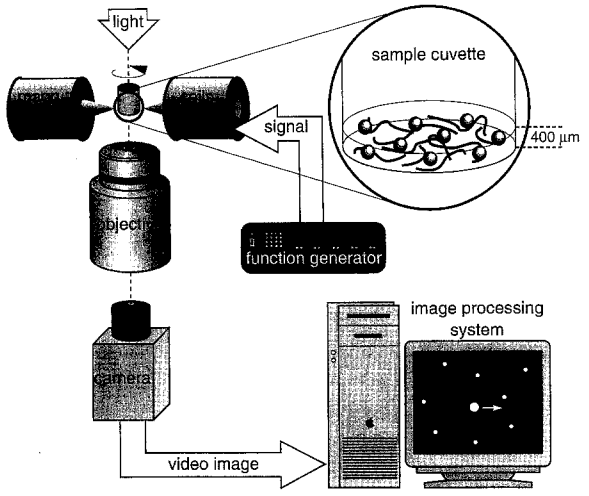

Fig. 1 Schematic view of the improved version of the magnetic bead micro-rheometer described in Ziemann et al. (1994). The rheometer is mounted on a Zeiss Axiovert microscope. Larger magnetic coils (diameter: 2 cm; length: 4 cm; 1600 turns of 0.35 mm copper wire) with tipped soft iron cores have been built to increase the magnetic field and to allow oil immersion microscopy for fluorescence experiments. The sample cells are cylindric plexiglass tubes of 8 mm diameter with a round cover slip as bottom (see magnification). The sample cell can be rotated about its long axis in order to apply forces in any direction in the x,y-plane (cf. Fig. 4). The function generator produces transient voltage pulses which are amplified and transferred to the coils

tion in Fig. 1) is confined by round cover slips which are held apart at a distance of about 400 µm using a teflon ring as spacer. Only beads located in the middle between top and bottom of the compartment were evaluated. The sample cell can be rotated about its long axis in order to apply forces in any direction in the x,y-plane. The signal generator produces transient voltage pulses which are amplified and transferred to the coils.

Images were taken with a Zeiss ×32, NA 0.4 objective using an additional ×2.5 magnification and a CCD camera (Hamamatsu, Herrsching, Germany). To track the positions of the beads in the x,y-plane, the video images were digitised with an Apple Macintosh Quadra 950 (Apple Computer) equipped with a Pixel-Pipeline frame-grabber card (Perceptics, Knoxville, TN). The following correlation analysis of a time series showing the movement of the bead was applied: The first video image (at $t=0$) was correlated with subsequent images (at $t=\tau_i$) taken at incremental time steps of $\Delta\tau_i=0.2$ sec. The coordinates of the maxima of each of the two-dimensional correlation functions $\langle G(\vec{x}, t=0)\cdot G(\vec{x}, t=\tau_i)\rangle$ were used to determine the displacement $\vec{u}(t)$ of the bead relative to the origin of the motion, where $G(\vec{x}, t)$ is the grayscale value at position $\vec{x}$ of the video image at time t. The correlation functions were determined by two-dimensional Fast Fourier Transform analysis. This program runs as a plug-in of the public domain image analysis software NIH Image (National Inst. of Health, Bethesda, MA). By using this technique, we achieve a spatial resolution of about 0.1 µm corresponding to the size of one pixel of the digitised images.

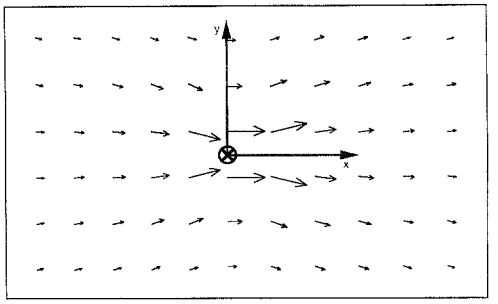

Fig. 2 Representation of shear field of an elastic body (given by Eq. 1) deformed by a local force in x-direction at center (⊗)

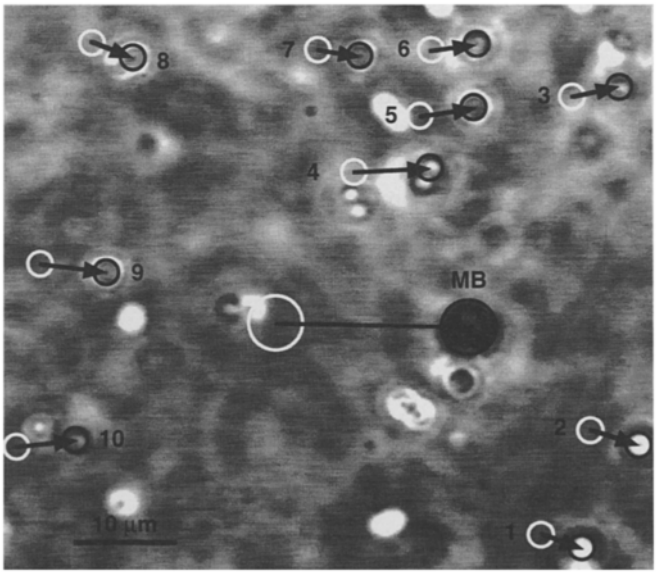

Fig. 3 Visualisation of local shear field in an actin network of monomer concentration $c_A \approx 0.12$ mg/ml (corresponding to a mesh size $\zeta \approx 1$ µm) contaminated by cross-linking protein. The phase contrast image shows the final positions of the 4.5 µm magnetic bead (denoted by MB) and the 2 µm non-magnetic beads (denoted with numbers 1 to 10). The initial and final positions of the beads are marked by white and black circles, respectively. For further clarification the initial and final positions are connected by arrows pointing in the direction of movement

Evaluation of experiments

To visualise the shear field within an cross-linked actin network, we embed paramagnetic and non-magnetic latex beads (cf. Materials and sample preparation) in the network. The magnetic beads are displaced by application of a constant force using magnetic tweezers. The resulting deformation field within the network can then be visualised by tracking the positions of the non-magnetic particles surrounding one magnetic bead in the field of view of the microscope.

In principle, quantitative evaluation of the experiments is based on the simplifying assumption that the deformation within the network can be described by the shear field generated by application of a point force within an infinite

elastic medium. This strain field can then be compared with the deformation field derived by tracking the motion of several non-magnetic beads.

Since the magnetic beads are small compared to the length scale of the measuring cell, the deformation field corresponds to that generated by a point force $\vec{f}$ in an infinite medium. The deformation field exhibits cylinder symmetry and is given by

$$\vec{u} = \frac{1+\sigma}{8\pi E(1-\sigma)} \cdot \frac{(3-4\sigma)\vec{f} + \vec{n}(\vec{n}\cdot\vec{f})}{r} \quad (1)$$

(Landau and Lifshitz 1959, vol. 7, ch. 8), where r is the distance from the point source, $\vec{n}$ denotes a normal in the direction of $\vec{r}$, σ the Poisson ratio and E the elastic constant. This vector field is represented in Fig. 2. The elastic parameters σ and E may be determined either by simulation of the elastic shear field and fitting to the experimental deflections of the non-magnetic beads or by evaluation of the latter on the basis of the following simple relationships:

1) The ratio β of the components of the deflections parallel (u_x) and perpendicular (u_y) to the force direction (ϑ is the angle between $\vec{r}$ and $\vec{f}$)

$$\beta = \frac{u_x}{u_y} = \frac{(3-4\sigma)+\cos^2\vartheta}{\sin\vartheta\cdot\cos\vartheta}, \quad (2)$$

2) the absolute value of the deflection

$$u = \sqrt{u_x^2+u_y^2} = \frac{f(1+\sigma)\sqrt{(3-4\sigma)^2+(7-8\sigma)\cos^2\vartheta}}{8\pi r E(1-\sigma)}. \quad (3)$$

The first relationship may be applied to measure local values of the Poisson ratio, σ, and the second for the determination of the elastic constant since the value of the force acting on a magnetic bead is known from a calibration of the magnetic tweezers that was performed as described previously (Ziemann et al. 1994). Finally, it is possible to derive the shear modulus using the equation

$$\mu = \frac{E}{2(1+\sigma)}.$$

Materials and sample preparation

The magnetic beads (Dynabeads, Dynal, Hamburg, Germany) used here were spherical latex particles (diameter $d=4.5$ μm) with an iron content of about 20% (w/w) (Door et al. 1991). The non-magnetic latex beads (Polybeads, Polysciences, Eppelheim, Germany) had diameters of 2 μm and 6 μm.

Monomeric actin, disassembly buffer (G-buffer) and polymerisation buffer (F-buffer) were prepared as described previously (Ruddies et al. 1993). The 120 kD gelation factor (cf. Schleicher et al. 1984), a homo-dimer, was prepared and provided by Prof. M. Schleicher (Institute for Cell Biology, University of Munich).

The cross-linked actin gel with embedded magnetic and non-magnetic beads was prepared as follows: 120 kD gelation factor, 4.5 μm-Dynabeads (approximately 10^5 beads/ml) and Polybeads (approximately 10^8 beads/ml of the 2 μm-beads and 10^7 beads/ml of the 6 μm-beads) were added to a G-actin solution which was then polymerised in F-buffer for 12 h at 4 °C.

Shear field mapping using non-magnetic 2 μm-beads as probes

In Fig. 3 we show the positions of the magnetic bead (denoted by MB) and ten probe beads (denoted by numbers 1 to 10) embedded in a F-actin gel at the beginning and end, respectively, of a force pulse of $f_0=10$ pN applied for 7 seconds. The magnetic bead (diameter 4.5 μm) acted as force transducer and the non-magnetic beads (diameter 2 μm) as probes. The initial and final positions of the beads are marked by white and black circles, respectively. For further clarification these positions are also connected by arrows.

Comparison of this micrograph with the strain field generated by a point force in an infinite elastic medium (Fig. 2) shows close agreement which allows a quantitative determination of local values of Poisson ratio and elastic constant. The detailed analysis is described in the next section.

The actin monomer concentration in this experiment was about $c_A=0.12$ mg/ml, corresponding to a mesh size of $\xi\approx 1$ μm (Schmidt 1988). The concentration of crosslinking proteins is not known. But crosslinking proteins have to be present for the following consideration: Assuming a reasonable value for the Poisson ratio of 0.5 (see below) we derive an elastic constant $E\approx 0.03$ Pa using the procedure described in the next section.

The value of the elastic constant should be compared with the plateau value, G_N^0, of the viscoelastic storage modulus, $G'(\omega)$, obtained in previous frequency dependent measurements of viscoelastic properties because the solution behaves as an elastic solid in this frequency regime. In contrast to $E\approx 0.03$ Pa, for a F-actin solution of concentration $c_A=0.1$ mg/ml $G_N^0\approx 0.01$ Pa was found (Müller et al. 1991; it should be noted that a recalibration of the oscillating disk rheometer used in this work (Müller 1991) showed that the values reported in this article are too large by a factor of about 20). The difference between E and G_N^0 can be accounted for by assuming that the network contains a small amount of a strongly binding cross-linking protein, such as filamin at an actin-to-cross-linker molar ratio of only $r_{AC}=500{:}1$. The presence of filamin at a concentration like this results in an increase of G_N^0 by a factor of about 4 (Ruddies et al. 1992). This example shows that the present microrheological technique allows the detection of very small amounts of cross-linking proteins and thus is a useful tool to test the purity of actin preparations.

Shear field mapping and evaluation of elastic parameters using non-magnetic 6 μm-beads as probes

Figure 4 shows a representative experiment for the local measurement of the strain field in an actin solution cross-

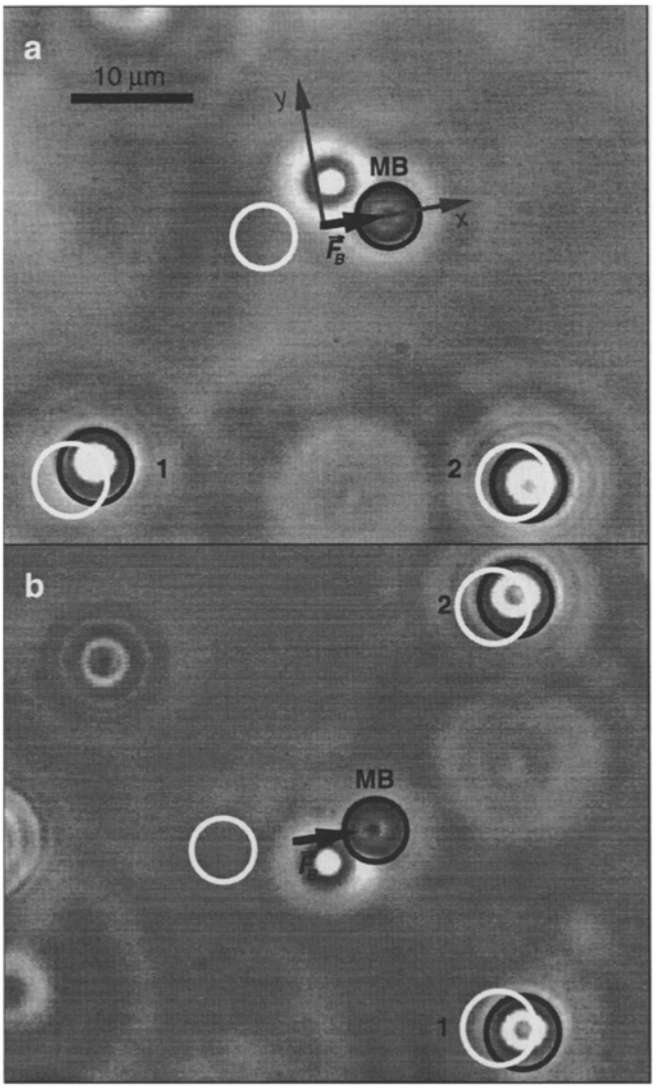

Fig. 4 a, b Measurement of local shear field by analysis of trajectories of non-magnetic beads (diameter 6 µm) in an actin network of monomer concentration $c_A = 0.14$ mg/ml (corresponding to a mesh size $\zeta = 1$ µm), cross-linked by 120 kD gelation factor at a cross-linker-to-actin molar ratio of $r_{CA} = 1{:}100$ (referred to the cross-linker monomer). The two phase contrast images show the final positions of the 4.5 µm magnetic bead (MB) and the 6 µm non-magnetic beads (denoted with numbers *1* and 2) observed for deflections of the magnetic bead in two perpendicular directions (**a** *x*-direction, **b** *y*-direction). Experiment **b** was performed after rotating the sample cell by 90°. The initial and final positions of the beads are marked by white and black circles, respectively. Note that the deflection of the magnetic bead (MB) is much larger than that of the probe beads (showing that the shear field of a point force inside of a cross-linked actin network decays rapidly)

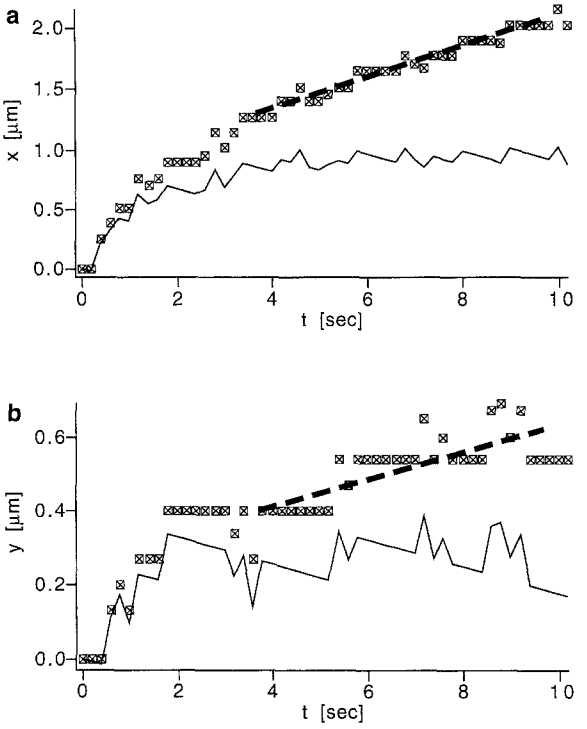

Fig. 5 a, b Analysis of time dependence of deflection of a non-magnetic bead in *x*-direction (**a**) and *y*-direction (**b**) by assuming that the shear strain is composed of an elastic and a viscous contribution. *Symbols* (⊠) measured positions; *drawn curves:* elastic contribution to the deflection of a non-magnetic bead obtained by subtraction of constant bead-velocity (corresponding to viscous flow). The latter velocity is derived from the slope of the dashed line which is obtained by fitting the experimental data at large time ($t > 4$ s)

linked by the 120 kD-gelation factor. Similar behaviour of the beads was found in experiments of the same kind that were performed in samples of the same composition with actin from different preparations. Magnetic beads with a diameter of 4.5 µm are embedded as force transducers and colloidal 6 µm-beads as non-magnetic probes. The actin monomer concentration was $c_A = 0.14$ mg/ml corresponding to a mesh size of $\xi \approx 1$ µm. The critical monomer concentration of actin is about 0.015 mg/ml (Piekenbrock and Sackmann 1992) and thus the G-actin fraction is only 10% of the total actin concentration. The actin-to-cross-linker molar ratio was $r_{AC} = 100{:}1$ (referred to the cross-linker monomer), corresponding to an average distance of the cross-linker along the actin chain of $\lambda \approx 0.6$ µm (note that the cross-linker in its active form is a dimer). The positions of the magnetic bead and two probe beads (denoted by numbers 1 and 2) are shown at the beginning and end, respectively, of a force pulse of $f_0 = 8$ pN applied for 10 seconds. The force has been applied in two perpendicular directions which was achieved by rotating the cuvette with respect to the magnetic field (cf. Fig. 1).

Figure 5 shows distance vs. time-plots of a non-magnetic probe bead in the direction parallel and perpendicular to the direction of strain. Clearly the probe beads are deflected both in a direction parallel (x) and perpendicular (y) to the applied force. The x-t- and y-t-plots are obtained by tracking the beads shown in Fig. 4 by using the two-dimensional correlation analysis described above. The strong fluctuations of the trajectories are mainly due to the Brownian motion of the non-magnetic beads while the step-like appearance of the trajectories is due to the limited resolution of the image processing software.

Table 1 Values of β and u (defined by Eqs. 2 and 3) for the experiments shown in Fig. 4, obtained from analysis of the elastic component of shear strain in x- and y-direction after displacement of the magnetic bead in two perpendicular directions in the x,y-plane. The last three rows present the calculated values of the Young modulus E, the Poisson ratio σ and the shear modulus $\mu = \frac{E}{2(1+\sigma)}$

	Fig. 4a, bead 1	Fig. 4a, bead 2	Fig. 4b, bead 1	Fig. 4b, bead 2
u [μm]	0.61	0.72	0.83	0.85
β	4.0	3.3	3.2	5.1
σ	0.42	0.44	0.47	0.25
E [10^{-2} Pa]	8.0	6.5	7.5	5.8
μ [10^{-2} Pa]	2.8	2.3	2.6	2.0

According to Fig. 5 all shear strain curves $x(t)$ and $y(t)$ can be well represented by superposition of an elastic strain $x_{el}(t)$ exhibiting saturation and a steady state flow with constant velocity v_c: $x(t)=x_{el}(t)+v_c \cdot t$. Without cross-linker one would not observe a considerable deflection of the non-magnetic beads as was tested in a separate experiment with a pure F-actin sample (data not shown). The finding of a residual viscous flow is a consequence of the fact that the network is still below the true gel point (cf. Sackmann 1994). The two contributions can be separated by first determining v_c from the limiting slope of the $x(t)$-curve at large time using least square fit (cf. the dashed line in Fig. 5) and subsequent subtraction of $v_c t$ from the experimental data (cf. the drawn curve in Fig. 5). The saturation value of the elastic contribution to the motion of the non-magnetic beads is further used for the calculation of the shear modulus and Poisson ratio as shown below.

In Table 1 the measured values of β and u for the beads shown in Fig. 4 are presented together with the calculated values of σ, E and μ. The values agree rather well showing that the network is on the average homogeneous over distances of at least 30 μm. The variations of σ are comparable to the measuring errors. However, they could also indicate local fluctuations in the network elasticity.

According to Table 1, the elastic modulus varies from $E=0.06$ Pa to $E=0.08$ Pa with an average value of $\bar{E}=0.07$ Pa. The average value for the Poisson ratio is $\bar{\sigma}=0.4$ from which an average shear modulus of $\bar{\mu}=\bar{E}/2(1+\bar{\sigma})\approx 0.03$ Pa can be deduced. The value of the elastic constant from the static experiment described here can again be compared with G_N^0. It agrees reasonably well with values of G_N^0 found by measurements with a rotational rheometer (Müller et al. 1991): For a network of monomer concentration $c_A=0.3$ mg/ml (mesh size $\xi\approx 0.7$ μm) without cross-linker G_N^0 is about 0.04 Pa, whereas for a network of the same actin-concentration at an actin-to-cross-linker molar ratio of $r_{AC}\approx 150{:}1$ G_N^0 is about 0.35 Pa. The Poisson ratio is close to the absolute upper bound $\sigma=0.5$ with exception of the value for bead 2 in Fig. 4b. A value of σ close to 0.5 is characteristic for polymer networks or polymer melts [$\sigma=0.5$ for natural rubber or $\sigma=0.49$ for low density polyethylene (Elias, 1971)]. The small value found for bead 2 in Fig. 4b is most likely an effect of the heterogeneity of the network.

Concluding remarks

We demonstrate that by the application of magnetic tweezers in combination with embedding of non-magnetic colloidal probes into the polymer solutions, local viscoelastic properties of actin networks and their spatial variations may be quantitatively evaluated.

By high precision analysis of the trajectories of non-magnetic beads using dynamic image processing, the shear modulus and Poisson ratio of cross-linked networks may be measured as a function of distance and orientation with respect to the point force within the network. The deflection-versus-time-curves for both directions ($x(t)$ and $y(t)$) may be described in terms of superpositions of purely elastic and purely viscous strain fields.

The above considerations show that the present local deformation technique enables reliable local measurements of viscoelastic parameters. This is astonishing since the local force field is composed of an elastic field and a flow field. The elastic field is given by Eq. 1 while the flow field generated by a bead comprises a component decaying linearly with the distance (as the force field) and a fast decaying part $\vec{v} \propto r^{-3}$ (cf. Landau and Lifshitz 1959, vol. 6, ch. 20). The latter is only dominant very close to the surface of the sphere. The linearly decaying component (which dominates at large distances), however, exhibits the same spatial symmetry as the elastic force field (cf. Eq. 1) and the colloidal probes are therefore deflected in the same direction by the two fields. Thus, the absolute values of the shear modulus obtained by application of Eq. 1 could be wrong at most by a factor of 2. More experiments are required to clarify this point.

The novel method for the visualisation and quantitative evaluation of shear fields in gels could in principle also be applied to denser polymer networks or cells, provided higher magnetic forces can be generated. Recent progress in the design of a modified type of setup allows application of up to 10 nN on magnetic beads of a diameter of 2.8 μm.

Acknowledgements We thank Dr. Marcus Ziegler for providing the image correlation analysis software. We are also very grateful to Prof. M. Schleicher (University of Munich) for the gift of the 120 kD gelation factor. Furthermore we acknowledge the financial support by the Deutsche Forschungsgemeinschaft (SFB 266) and the Fonds der Chemischen Industrie. The work was also partially supported by the National Science Foundation under grant number PHY8904035. Last not least one of the authors (E.S.) gratefully acknowledges the hospitality of the Institute for Theoretical Physics of the University of California Santa Barbara where part of this work was written.

References

Darnell J, Lodish H, Baltimore D (1990) Molecular cell biology. Scientific American Books, New York

Door R, Frösch D, Martin R (1991) Estimation of section thickness and quantification of iron standards with EELS. J Microsc 162:15–22

Elias HG (1971) Makromoleküle. Struktur, Eigenschaften, Synthesen, Stoffe. Hüthig & Wepf, Basel

Evans E, Ritchie K, Merkel R (1995) Sensitive force technique to probe molecular adhesion and structural linkages at biological interfaces. Biophys J 68:2580–2587

Finer JT, Simmons RM, Spudich JA (1994) Single myosin molecule mechanics: piconewton forces and nanometre steps. Nature 368:113–119

Ishijima A, Doi T, Sakurada K, Yanagida T (1991) Sub-piconewton force fluctuations of actomyosin in vitro. Nature 352:301–306

Kuo SC, Sheetz MP (1992) Optical tweezers in cell biology. TIBS 2:116–118

Landau LD, Lifshitz EM (1959) Course of theoretical physics, Vol 6. Fluid mechanics. Pergamon Press, London

Landau LD, Lifshitz EM (1959) Course of theoretical physics, Vol 7. Theory of elasticity. Pergamon Press, London

Müller O (1991) Entwicklung eines Rheometers zur Untersuchung viskoelastischer Eigenschaften membranassoziierter Aktinnetzwerke im verdünnten und halbverdünnten Bereich. Doctoral thesis, TU München

Müller O, Gaub HE, Bärmann M, Sackmann E (1991) Viscoelastic moduli of sterically and chemically cross-linked actin networks in the dilute to semi-dilute regime: measurements by an oscillating disk rheometer. Macromolecules 24:3111–3120

Piekenbrock T, Sackmann E (1992) Quasielastic light scattering study of thermal excitations of F-actin solutions and of growth kinetics of actin filaments. Biopolymers 32:1471–1489

Ruddies R, Goldmann WH, Isenberg G, Sackmann E (1992) The viscoelastic moduli of actin/filamin solutions: A micro-rheologic study. Biochem Soc Trans 21:37S

Ruddie R, Goldmann WH, Isenberg G, Sackmann E (1993) The viscoelasticity of entangled actin networks: the influence of defects and modulation by talin and vinculin. Eur Biophys J 22:309–321

Sackmann E (1994) Intra- and extracellular macromolecular networks: physics and biological function. Macromol Chem Phys 195:7–28

Schindl M, Wallraff E, Deubzer B, Witke W, Gerisch G, Sackmann E (1995) Cell-substrate interactions and locomotion of *dictyostelium* wild-type and mutants defective in three cytoskeletal proteins: a study using quantitative reflection interference contrast microscopy. Biophys J 68:1177–1190

Schleicher M, Gerisch G, Isenberg G (1984) New actin-binding proteins from *dyctostelium discoideum*. EMBO (Eur Mol Biol Organ) J 3:2095–2100

Schmidt C (1988) Struktur und Dynamik polymerer Aktinnetzwerke und ihre Wechselwirkung mit Modellmembranen. Doctoral thesis, TU München

Stossel TP (1994) The machinery of cell crawling. Sci Amer 271 (3):54–55, 58–63

Svoboda K, Schmidt CF, Schnapp BJ, Block SM (1993) Direct observation of kinesin stepping by optical trapping interferometry. Nature 365:721–727

Wachsstock DH, Schwarz WH, Pollard TD (1993) Affinity of α-actinin for actin determines the structure and mechanical properties of actin filament gels. Biophys J 65:205–214

Wang N, Butler JP, Ingber DE (1993) Mechanotransduction across the cell surface and through the cytoskeleton. Science 260:1124–1127

Zaner KS, Valberg PA (1989) Viscoelasticity of F-actin measured with magnetic microparticles. J Cell Biol 109:2233–2243

Ziemann F, Rädler J, Sackmann E (1994) Local measurements of viscoelastic moduli of entangled actin networks using an oscillating magnetic bead microrheometer. Biophys J 66:2210–2216